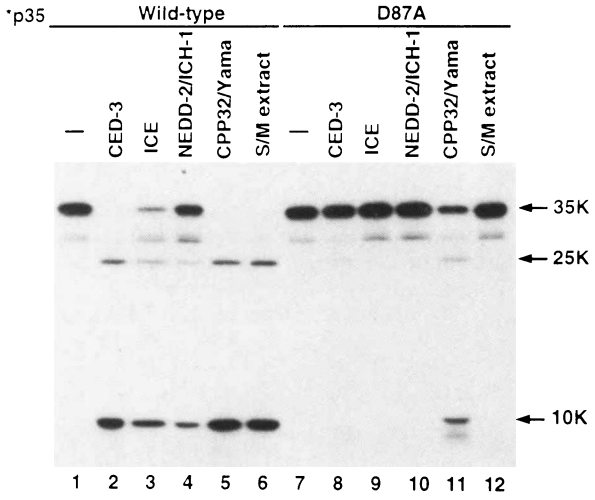

FIG. 3 p35 is a substrate of murine ICE, human NEDD-2/ICH-1, human CPP32/Yama and chicken S/M extract. ^{35}S-methionine-labelled p35 proteins (*p35) were incubated with 40 ng purified protease for 20 min at 30 °C. Lanes 1–6, wild-type p35; lanes 7–12, mutant p35D87A; lanes 1 and 7, CED-3 buffer; lanes 2 and 8, purified CED-3 protease (40 ng); lanes 3 and 9, purified murine ICE protease (40 ng); lanes 4 and 10, purified human NEDD-2/ICH-1 protease (40 ng); lanes 5 and 11, purified human CPP32/Yama protease (40 ng); lanes 6 and 12, 1 μl chicken S/M extract[23].

did not generate a functional cell-death inhibitor, it is conceivable that such an inhibitor can be made only by proteolysis of an intact protein. Alternatively, the CED-3/ICE cleavage site in p35 could act by allowing p35 to bind to the active site of, and thereby competitively inhibit, these proteases. If present at relatively high levels, p35 could inhibit by mass action; appropriately high levels of p35 expression might be obtained normally as a consequence of viral infection, and in cell culture and in the worm as a consequence of expression from strong promoters. If cleaved relatively inefficiently, p35 could inhibit by prolonged association with the proteases. We further suggest that crmA, or any other exogenous or endogenous substrates of members of the CED-3/ICE cysteine protease family, might similarly function as competitive inhibitors of these enzymes and hence of programmed cell death. □

Received 18 July; accepted 30 August 1995.

1. Clem, R. J., Fechheimer, M. & Miller, L. K. *Science* **254,** 1388–1390 (1991).
2. Rabizadeh, S., LaCount, D. J.. Friesen, P. D. & Bredesen, D. E. *J. Neurochem.* **61,** 2318–2321 (1993).
3. Sugimoto, A., Friesen, P. D. & Rothman, J. H. *EMBO J.* **13,** 2023–2028 (1994).
4. Hay, B. A., Wolff, T. & Rubin, G. M. *Development* **120,** 2121–2129 (1994).
5. Martinou, I. *et al. J. Cell Biol.* **128,** 201–208 (1995).
6. Ellis, H. M. & Horvitz, H. R. *Cell* **44,** 817–829 (1986).
7. Yuan, J., Shaham, S., Ledoux, S., Ellis, H. M. & Horvitz, H. R. *Cell* **75,** 641–652 (1993).
8. Thornberry, N. A. *et al. Nature* **356,** 768–774 (1992).
9. Cerretti, D. P. *et al. Science* **256,** 97–100 (1992).
10. Miura, M., Zhu, H., Rotello, R., Hartweig, E. A. & Yuan, J. *Cell* **75,** 653–660 (1993).
11. Fernandes-Alnemri, T., Litwack, G. & Alnemri, E. S. *J. biol. Chem.* **269,** 30761–30764 (1994).
12. Wang, L., Miura, M., Bergeron, L., Zhu, H. & Yuan, J. *Cell* **78,** 739–750 (1994).
13. Kumar, S., Kinoshita, M., Noda, M., Copeland, N. G. & Jenkins, N. A. *Genes Dev.* **8,** 1613–1626 (1994).
14. Tewari, M. *et al. Cell* **81,** 801–809 (1995).
15. Ray, C. A. *et al. Cell* **69,** 597–604 (1992).
16. Gagliardini, V. *et al. Science* **263,** 826–828 (1994).
17. Tewari, M. & Dixit, V. M. *J. biol. Chem.* **270,** 3255–3260 (1995).
18. Enari, M., Hug, H. & Nagata, S. *Nature* **375,** 75–81 (1995).
19. Los, M. *et al. Nature* **375,** 81–83 (1995).
20. Smith, D. B. & Johnson, K. S. *Gene* **67,** 31–40 (1988).
21. Friesen, P. D. & Miller, L. K. *J. Virol.* **61,** 2264–2272 (1987).
22. Howard, A. D. *et al. J. Immun.* **147,** 2964–2969 (1991).
23. Lazebnik, Y. A., Kaufmann, S. H., Desnoyers, S., Poirier, G. G. & Earnshaw, W. C. *Nature* **371,** 346–347 (1994).
24. Stringham, E. G., Dixon, D. K., Jones, D. & Candido, E. P. *Molec. Biol. Cell* **3,** 221–233 (1992).
25. Hengartner, M. O. & Horvitz, H. R. *Cell* **76,** 665–676 (1994).
26. Komiyama, T. *et al. J. biol. Chem.* **269,** 19331–19337 (1994).
27. Molineaux, S. M. *et al. Proc. natn. Acad. Sci. U.S.A.* **90,** 1809–1813 (1993).
28. Sambrook, J., Fritsch, E. F. & Maniatis, T. *Molecular Cloning: A Laboratory Manual* (Cold Spring Harbor Lab. Press, NY, 1989).
29. Kunkel, T. A. *Proc. natn. Acad. Sci. U.S.A.* **82,** 488–492 (1985).
30. Chiang, C. M. & Roeder, R. G. *Peptide Res.* **6,** 62–64 (1993).

ACKNOWLEDGEMENTS. We thank T. Baker, B. Conradt, S. van den Heuvel, M. Koelle, H. Sawa and S. Shaham for discussions; J. Yuan for providing complementary DNAs encoding murine ICE, human ICH-1 and cowpox virus crmA; A. Sugimoto, P. D. Friesen and J. H. Rothman for a cDNA encoding baculovirus p35; Y. Lazebnik for chicken S/M extract; A. Fire for the heat-shock vectors; S. Desnoyers and G. G. Poirier for a cDNA encoding human PARP; E. Hartwieg for help with photography; and the MIT Biopolymers Laboratory for the microsequencing analysis. D.X. was supported by postdoctoral fellowships from the Anna Fuller Fund and the Helen Hay Whitney Foundation. H.R.H. is an Investigator of the Howard Hughes Medical Institute.

Unbinding force of a single motor molecule of muscle measured using optical tweezers

Takayuki Nishizaka*, Hidetake Miyata†, Hiroshi Yoshikawa†, Shin'ichi Ishiwata*‡§ & Kazuhiko Kinosita Jr†

* Department of Physics, School of Science and Engineering, and ‡ Advanced Research Center for Science and Engineering, Waseda University, 3-4-1 Okubo, Shinjuku-ku, Tokyo 169, Japan
† Department of Physics, Faculty of Science and Technology, Keio University, 3-14-1 Hiyoshi, Kohoku-ku, Yokohama 223, Japan

THE unbinding and rebinding of motor proteins and their substrate filaments are the main components of sliding movement[1]. We have measured the unbinding force between an actin filament and a single motor molecule of muscle, myosin, in the absence of ATP, by pulling the filament with optical tweezers[2]. The unbinding force could be measured repeatedly on the same molecule, and was independent of the number of measurements and the direction of the imposed loads within a range of ±90°. The average unbinding force was 9.2 ± 4.4 pN, only a few times larger than the sliding force[3–5] but an order of magnitude smaller than other intermolecular forces[6,7]. From its kinetics[8] we suggest that unbinding occurs sequentially at the molecular interface, which is an inherent property of motor molecules.

In the absence of ATP, a myosin molecule binds to an actin filament forming a crossbridge through a rigor bond. On a glass surface coated with a low concentration of heavy meromyosin (HMM), which is a proteolytic fragment of myosin, short actin filaments (1–2 μm long) rotated around a single point over a range of more than 360° (which is analogous to a microtubule tethered by a single kinesin molecule[9]). Long filaments (5–20 μm long) were attached to the surface at nodal points a few micrometres apart (Fig. 1), between which the filament showed brownian bending motion. These observations suggest that each attachment point corresponds to a single HMM molecule[10], although it is possible that a cluster of HMM molecules may have been involved in some cases.

To measure the unbinding force needed to rupture the rigor bond, we used optical tweezers to impose an external load on the crossbridge by manipulating a polystyrene bead attached to the rear end of an actin filament using gelsolin, an actin binding protein (Fig. 1). The actin filament, once detached, could be reattached by manipulating it into the same position on the surface, provided the front remained attached to the surface by one or more HMM molecules. The reattachment was usually made at a slightly different point on the actin filament indicating

§ To whom correspondence should be addressed.

that the unbinding had occurred between the actin filament and the HMM molecule, not between the HMM molecule and the glass surface.

The time course of the displacement of the bead is shown in Fig. 2*a*. First, the bead smoothly followed a laser spot moving at a constant rate (along the dotted line), but lagged behind after the actin filament became taut (at 1.4 s; compare with Fig. 1*A*, *a*), so that a load proportional to the distance between the bead and the trap centre was imposed on the rigor bond (labelled 'stress' in Fig. 2*a*). When the rigor bond was ruptured, the bead returned to the trap centre (at 2.9 s in Fig. 2*a*; compare with Fig. 1*A*, *b*), and we could directly determine the unbinding force from this abrupt displacement. The distribution of this unbinding force is shown in Fig. 2*c*: the peak was at 7 pN and the mean value was 9.2 ± 4.4 pN ($n = 168$). This unbinding force is much smaller than other intermolecular forces, for example 110 pN for actin–actin[6], 160 pN for avidin–biotin[7] and >20 pN for actin–gelsolin (judging from the stability observed in the above measurements), but is comparable to the maximum sliding force produced by a single HMM molecule in the presence of ATP[3–5].

Even after the actin filament became taut, the bead was displaced slightly ('strain' in Fig. 2*a*), such that a stress–strain relation could be obtained (Fig. 2*b*). The maximum strain at which the rigor bond was ruptured was 69 ± 27 nm ($n = 30$), larger than a myosin head (20 nm), which indicates that the strain contains

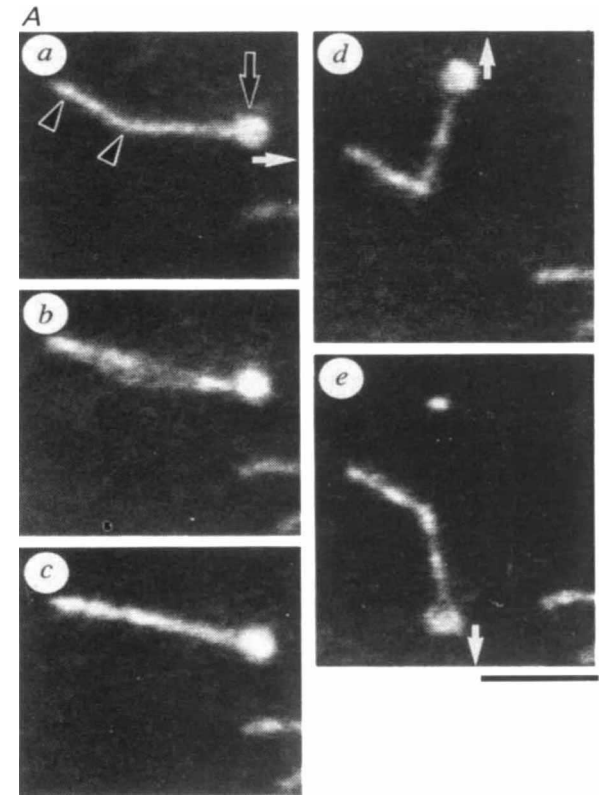

FIG. 1 *A*, A series of fluorescence micrographs showing the measurement of the unbinding force of a rigor bond(s) between a single actin filament and a single HMM molecule. The bead (indicated by the black arrow in *a*) was trapped by a single beam of laser light and moved at a constant rate to the direction indicated by the white arrow, such that the actin filament became taut. The actin filament was attached to the surface by two separate HMM molecules identified as two nodal points (arrowheads in *a*)[10]. As the laser spot was further moved, the load was increased and subsequently one of the two molecules unbound (*b*), such that the filament became nearly straight (*c*). The actin filament could be reattached to the same HMM molecule repeatedly by manipulating the filament into the same position while the second molecule was still attached, and the external loads could be imposed in any direction, as indicated by the white arrows (*d* and *e*). Scale bar, 5 μm. *B*, Schematic illustration of *A*: θ is the angle of the applied force, h (<1 μm) is the height of the bead ($\phi \leqslant 10°$).

METHODS. Actin and myosin were prepared from rabbit skeletal white muscle. HMM prepared by chymotryptic digestion of myosin was stored in liquid N_2 (ref. 18). Gelsolin was prepared as described previously[19] and crosslinked to the carboxylated polystyrene bead (1 μm in diameter; Polysciences, PA) with 1-ethyl-3-(3-dimethylaminopropyl)-carbodiimide (N. Suzuki *et al.*, submitted), such that the barbed end of an actin filament was attached to the bead. The average number of actin filaments attached to the bead was controlled by crosslinking an appropriate amount of bovine serum albumin (BSA) to the bead (for example, BSA:gelsolin = 20:1 in weight ratio). A small amount of BSA labelled with rhodamine X maleimide (Molecular Probes, Eugene, OR) was also crosslinked to the bead surface, and the actin filaments were labelled with rhodamine phalloidin (Molecular Probes). The *in vitro* assay system was based on that reported previously[20] but with modifications as follows: the coverslip was exposed to vaporized hexamethyl disilazane (HMDS; Nakalai Tesque, Kyoto) at room temperature overnight. A 50-μm thick flow cell, of which the lower surface was an HMDS-coated coverslip, was filled with assay buffer (25 mM KCl, 4 mM $MgCl_2$, 25 mM imidazole-HCl (pH 7.4), 1 mM EGTA, 1 mM dithiothreitol). Then 2–5 μg ml^{-1} HMM, in assay buffer, was infused from each side of the cell, at an interval of 60 s, and washed with assay buffer containing 0.5 mg ml^{-1} BSA, 10 mM dithiothreitol, 0.22 mg ml^{-1} glucose oxidase, 0.036 mg ml^{-1} catalase and 4.5 mg ml^{-1} glucose (solution B). Finally, bead-tailed actin filaments (20 nM actin and 0.05% (w/v) bead), in solution B, were infused. All experiments were done at 28–30 °C after rinsing the flow cell three times with solution B to wash out ATP ($\leqslant$20 nM) carried over from the G-actin solution. An inverted microscope (TMD-300: an oil-immersion objective lens with a phase ring, ×100 NA = 1.3; Nikon, Tokyo) was equipped with optical tweezers based on a 1 W Nd:YLF laser (1053–1000p: $\lambda = 1.053$ μm; Amoco Laser, IL). The linear polarization of the laser light was changed to circular using a quarter waveplate. The trap centre could be moved at a constant rate by controlling a movable mirror with d.c. servo-motors (optmike-e; Sigma Koki, Hidaka, Japan). A phase-contrast image of the bead was digitized and its centroid was calculated with a frame memory computer (DIPS-C2000; Hamamatsu Photonics, Hamamatsu, Japan). A fluorescent image of an actin filament was simultaneously acquired with a modified dual-view microscopy system[21,22]. The trap stiffness used was about 0.1 pN nm^{-1} (at a laser power of 95 mW without the objective) as measured by the following two distinct methods. First, the position of a bead undergoing thermal brownian motion around the trap centre at a low laser power, for example, 0.43 mW, was analysed at a shutter speed of 1/8,000 s with a non-interlace CCD camera (TM-9700; PULNiX, Kyoto). Assuming the Boltzmann distribution for the bead position, the trap stiffness was calculated as 0.44×10^{-3} pN nm^{-1}, corresponding to 0.097 pN nm^{-1} at 95 mW. The stiffness values thus estimated at $h = 0.5$, 1.5 and 2.5 μm coincided to within ±5%. Second, the flow cell was displaced at a constant rate using a substage with a piezoelectric transducer (L. Pickelmann, Munich, Germany). A bead, trapped at $h = 2.5$ μm so as to make the effects of viscous coupling to the glass surface negligible, was displaced owing to the viscosity of water. The displacement was proportional, to 200 nm, to the force calculated as $F = 6\pi\eta av$, where η is the viscosity of water, a is the radius of the bead (0.5 μm), and v is the velocity of the flow cell. The trap stiffness was 0.095 pN nm^{-1} at 95 mW.

© 1995 Nature Publishing Group

the elongation or tilting of some elastic parts in addition to a myosin head. It should be noted, however, that the average elastic modulus, 0.58 ± 0.26 pN nm^{-1} ($n = 17$), estimated at a stress of 8–10 pN (dotted line in Fig. 2*b*), was similar to the elastic modulus of a crossbridge estimated in muscle fibres[1,11].

We could repeatedly measure the unbinding force of the same HMM molecule by selecting long actin filaments attached to the glass surface at more than two points (Fig. 1); short filaments attached at a single point were difficult to reattach after unbinding because of extensive brownian motion at the free end. The unbinding force did not change significantly, even with repetition of the measurements (Fig. 3*a*), indicating that HMM had not been denatured despite the rigor bond being ruptured several times by the external loads.

We also examined whether the unbinding force depends on the direction of the external load (Fig. 1*Aa*, *d*, *e*). The angle (θ in Fig. 1*B*) was limited within the range of ±90°, because filaments forced to bend at angles larger than 90° tended to break at the bend. As shown in Fig. 3*b*, the unbinding force appeared to be independent of the direction of the load. This is due to the flexibility of an HMM molecule, as revealed by the rotation of the attached short actin filaments. In contrast, the sliding force[4] and velocity[12,13] of an actin filament depend largely on the orientation of myosin molecules assembled in a thick filament.

The lifetime of a rigor bond without a load has been reported to be 10^2–10^3 s (refs 14, 15). In our experiments (Fig. 2), HMM molecules detached within 3 s of an external load being imposed (1.5 (=2.9 − 1.4) in Fig. 2*a*), implying that the external load decreased the lifetime of the rigor bond. To confirm this load dependence, we applied a sudden, constant load and then measured the time that elapsed before unbinding occurred (Fig. 4). Individual lifetimes measured repeatedly on each HMM clearly show that a higher load tends to shorten the lifetime (see lines connecting the symbols in Fig. 4). This is consistent with the observation that the detachment rate of rigor crossbridges in muscle fibres is stress-sensitive[16]. Note that, although variations between different HMM molecules are large, data on individual HMM are relatively consistent (see also Fig. 3).

In our experiments, the actin filament was always 'pulled' in the direction opposite to the 'power stroke' of myosin (the bead being on the rear end of the actin filament), and the reverse pull at ~10 pN accelerated the rate of unbinding of the rigor bond by a factor of 10^2–10^3 (from 10^2–10^3 s to ~1 s (Figs 2 and 4)). This would imply an interaction distance of the order of (ln (10^2–10^3))$k_BT/10$ pN ~ (2–3) nm (where k_B is the Boltzmann constant and T the absolute temperature)[17], which is an order of magnitude greater than the length of individual bonds at the molecular

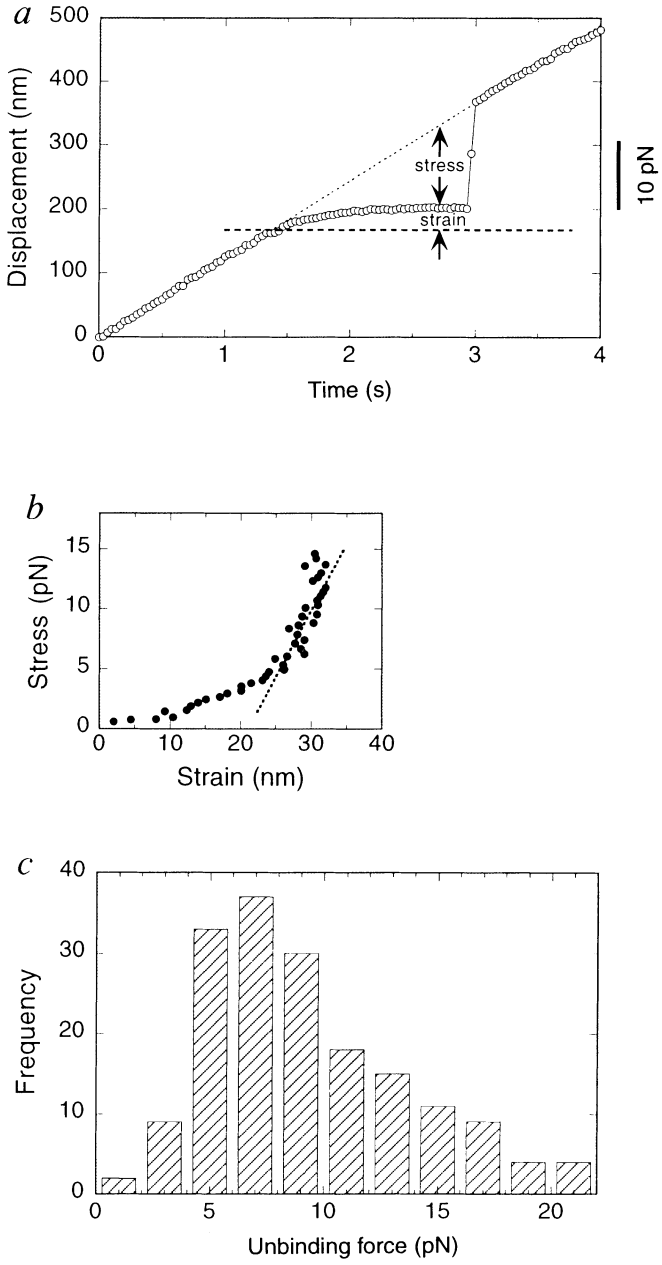

FIG. 2 *a*, Time course of the movement of the trap centre (dotted line, 120 nm s^{-1}, corresponding to about 12 pN s^{-1}) and the bead (circles) to which a single actin filament was attached. From the abrupt displacement at 2.9 s, when the rigor bond was ruptured, the unbinding force between an actin filament and an HMM molecule was estimated. *b*, Stress–strain relation obtained after the actin filament became taut at 1.4 s in *a*. In most samples the elastic modulus increased as the strain became large. The dotted line shows the elastic modulus at the imposed load of 8–10 pN. *c*, Histogram of the unbinding force between a single actin filament and a single HMM molecule.

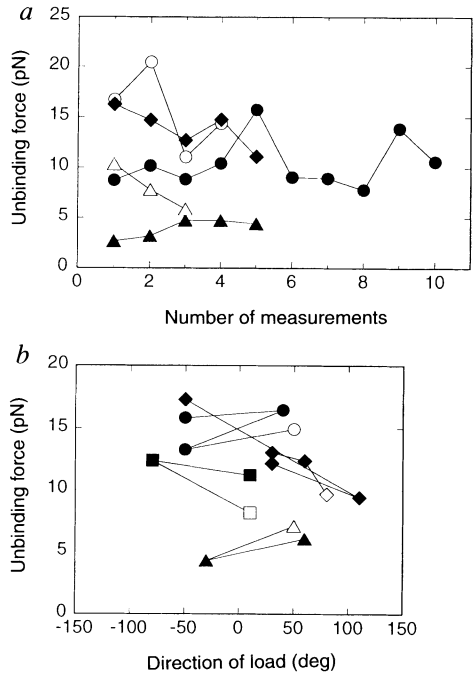

FIG. 3 Effects of the number of measurements (*a*) and the direction (θ defined in Fig. 1*B*) of the external loads (*b*) on the unbinding force measured on the same HMM molecules. Different symbols in each figure represent different HMM molecules. Open and closed symbols in *b* indicate the first and subsequent measurements, respectively, connected by lines.

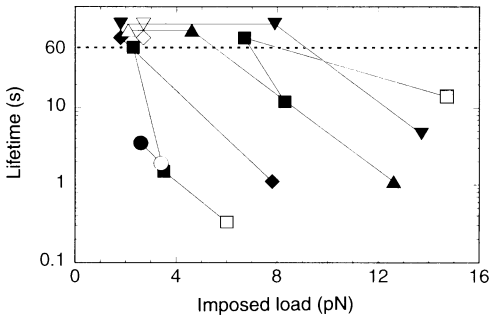

FIG. 4 Effects of the imposed loads on the lifetime of the rigor bond. The flow cell was displaced stepwise within 1/30 s so as to impose a constant external load (2–15 pN) using a piezoelectric substage (p-770.10; Physik Instrumente, Germany) with a function generator (1915; NF Electronic Instruments, Japan). The lifetime was repeatedly measured at various loads for the same HMM molecules. For those rigor bonds not ruptured within 60 s, the lifetimes are plotted above the broken line indicating 60 s. Different symbols represent different HMM molecules, and open and closed symbols indicate the first and subsequent measurements, respectively, connected by lines.

interface. On the other hand, the rate of unbinding of molecular bond(s) having a typical interaction distance (~0.3 nm) would be increased only by a factor of $2 \sim \exp(10\,\mathrm{pN} \cdot 0.3\,\mathrm{nm}/k_BT)$ (cf. Fig. 3 in ref. 8). This suggests that the reverse pull of the actin filament decreased very efficiently the activation energy barrier for unbinding.

Taken together, our results indicate that pulling an actin filament tends to distort the actin–myosin interface in such a way as to break the bonds at the interface sequentially from one end. This should be a rapid process compared to unbinding without a load, in which all bonds must break almost simultaneously. Conversely, if the myosin molecule in the 'power stroke' prestate could be 'pushed' in the direction of the 'power stroke', that is, towards the rigor-like state, a conformational change(s) that progressively increases the cohesive force between actin and myosin would occur and a longer lifetime would be expected. These properties were predicted on the basis of biochemical data, but our mechanical results suggest that they are inherent to the actin–myosin interaction, and that the role of ATP splitting regulate the process of conformational change. □

Received 23 January; accepted 31 July 1995.

1. Huxley, A. F. *Prog. Biophys. biophys. Chem.* **7,** 255–318 (1957).
2. Ashkin, A., Dziedzic, J. M., Bjorkholm, J. E. & Chu, S. *Optics Lett.* **11,** 288–290 (1986).
3. Finer, J. T., Simmons, R. M. & Spudich, J. A. *Nature* **368,** 113–119 (1994).
4. Ishijima, A. *et al. Biochem. biophys. Res. Commun.* **199,** 1057–1063 (1994).
5. Miyata, H. *et al. Biophys. J.* **68,** 286s–290s (1995).
6. Kishino, A. & Yanagida, T. *Nature* **334,** 74–76 (1988).
7. Florin, E., Moy, V. T. & Gaub, H. E. *Science* **264,** 415–417 (1994).
8. Erickson, H. P. *Proc. natn. Acad. Sci. U.S.A.* **91,** 10114–10118 (1994).
9. Hunt, A. J. & Howard, J. *Proc. natn. Acad. Sci. U.S.A.* **90,** 11653–11657 (1993).
10. Nishizaka, T., Miyata, H., Yoshikawa, H., Ishiwata, S. & Kinosita, K. Jr *Biophys. J.* **68,** 75s (1995).
11. Tawada, K. & Kimura, M. *J. Muscle Res. Cell Motil.* **7,** 339–350 (1986).
12. Yamada, A., Ishii, N. & Takahashi, K. *J. Biochem., Tokyo* **108,** 341–343 (1990).
13. Sellers, J. R. & Kachar, B. *Science* **249,** 406–408 (1990).
14. Marston, S. B. *Biochem. J.* **203,** 453–460 (1982).
15. Ishiwata, S. & Yasuda, K. *Phase Transitions* **45,** 105–136 (1993).
16. Schoenberg, M. & Eisenberg, E. *Biophys. J.* **48,** 863–871 (1985).
17. Bell, G. I. *Science* **200,** 618–627 (1978).
18. Nishizaka, T., Yagi, T., Tanaka, Y. & Ishiwata, S. *Nature* **361,** 269–271 (1993).
19. Kurokawa, H., Fujii, W., Ohmi, K., Sakurai, T. & Nonomura, Y. *Biochem. biophys. Res. Commun.* **168,** 451–457 (1990).
20. Toyoshima, Y. Y. *et al. Nature* **328,** 536–539 (1987).
21. Miyata, H. *et al. J. Biochem., Tokyo* **115,** 644–647 (1994).
22. Kinosita, K. Jr *et al. J. Cell Biol.* **115,** 67–73 (1991).

ACKNOWLEDGEMENTS. We thank N. Suzuki and I. Sase for technical assistance in the use of optical tweezers and dual-view microscopy, and T. Iga for preparing the gelsolin. This research was partly supported by Grants-in-Aid for Scientific Research and for Scientific Research on Priority Areas from the Ministry of Education, Science and Culture of Japan. T.N. is a recipient of a JSPS Fellowship for Japanese Junior Scientists.

A general mechanism for transcriptional synergy by eukaryotic activators

Tianhuai Chi*, Paul Lieberman†, Katharine Ellwood* & Michael Carey*‡

* Department of Biological Chemistry, University of California, Los Angeles, School of Medicine, 10833 LeConte Avenue, Los Angeles, California 90095-1737, USA
† Roche Institute of Molecular Biology, Department of Gene Expression, 340 Kingsland Street, Nutley, New Jersey 07110-1199, USA

One of the important regulatory concepts to emerge from studies of eukaryotic gene expression is that RNA polymerase II promoters and their upstream activators are composed of functional modules whose synergistic action regulates the transcriptional activity of a nearby gene[1–3]. Biochemical analysis of synergy by ZEBRA, a non-acidic activator of the Epstein–Barr virus (EBV) lytic cycle[4], showed that the synergistic transcriptional effect of promoter sites and activation modules correlates with assembly of the TFIID:TFIIA (DA) complex in DNase I footprinting and gel shift assays. The activator-dependent DA complex differs from a basal DA complex by its ability to bind TFIIB stably in an interaction regulated by TATA-binding protein-associated factors (TAFs). TFIIB enhances the degree of synergism by increasing complex stability. Similar findings were made with the acidic activator GAL4-VP16. Our data suggest a unifying mechanism for gene activation and synergy by acidic and non-acidic activators, and indicate that synergy is manifested at the earliest stage of preinitiation complex assembly.

ZEBRA (also called Zta) is known to stimulate assembly of the DA complex *in vitro*[1,5]. We reasoned that if this was indeed a biologically relevant event then it should be included in the mechanism of transcriptional synergy[6]. The electrophoretic mobility shift assay in Fig. 1*a* and the corresponding DNase I footprints in Fig. 1*b* demonstrate that ZEBRA strongly stimulated formation of DA complexes on two different core promoters bearing multiple upstream sites (3 and 7 sites: Z_3- and Z_7-E4T or -M), but did not alter the basal amount of complex formed on a template bearing a single site (Z_1). The results indicate that the site-dependent synergistic effect of ZEBRA observed in transcription assays *in vivo* and *in vitro*[1,7] (M.C. and T.C., unpublished observations) is first manifested at the DA complex and that the cooperativity is not restricted to a particular core promoter. Furthermore, synergistic DA recruitment occurs while the ZEBRA sites are saturated, which suggests that multiple molecules of activator are simultaneously interacting with DA, in accordance with a model we have proposed previously[8,9]. DNase I footprinting also showed that removing either of two non-acidic activation modules (regions I and II), which act synergistically to enhance ZEBRA's activity in transcription assays[1,7] (data not shown), abolishes formation of the DA complex (Fig. 1*c*), which is similar to the mutant's transcriptional effects. The ZEBRA-responsive DA footprint encompasses both the TATA box and downstream regions, generating an extended series of downstream enhancements and protections[10–12].

ZEBRA promotes binding of TFIIB to DA (Fig. 2). The gel shift in Fig. 2*a* shows that, although TFIIB had no discernible effect on the mobility or amount of basal DA complex (lanes 1 and 3), it generated a clear DAB supershift in the presence of

‡ To whom correspondence should be addressed.

© 1995 Nature Publishing Group